## HEALTH AND MEDICINE

# Anti-α4β7 monoclonal antibody–conjugated nanoparticles block integrin α4β7 on intravaginal T cells in rhesus macaques

Sidi Yang[1], Geraldine Arrode-Bruses[2], Ines Frank[2], Brooke Grasperge[3], James Blanchard[3], Agegnehu Gettie[4], Elena Martinelli[2]*†, Emmanuel A. Ho[1]*†

Intravenous administration of anti-α4β7 monoclonal antibody in macaques decreases simian immunodeficiency virus (SIV) vaginal infection and reduces gut SIV loads. Because of potential side effects of systemic administration, a prophylactic strategy based on mucosal administration of anti-α4β7 antibody may be safer and more effective. With this in mind, we developed a novel intravaginal formulation consisting of anti-α4β7 monoclonal antibody–conjugated nanoparticles (NPs) loaded in a 1% hydroxyethylcellulose (HEC) gel (NP-α4β7 gel). When intravaginally administered as a single dose in a rhesus macaque model, the formulation preferentially bound to CD4+ or CD3+ T cells expressing high levels of α4β7, and occupied ~40% of α4β7 expressed by these subsets and ~25% of all cells expressing α4β7. Blocking of the α4β7 was restricted to the vaginal tract without any changes detected systemically.

## INTRODUCTION

Integrins are a group of transmembrane cell adhesion receptors that facilitate cell attachment to extracellular ligands and trigger intracellular signaling pathways (1). The integrin family consists of 24 heterodimeric proteins, and each protein contains α and β subunits that are noncovalently bonded together (1). Integrin α4β7 (α4β7) is a gut mucosal homing receptor that is responsible for peripheral T cell homing into gut-associated lymphoid tissues (GALT) through the interaction with mucosal vascular addressin cell adhesion molecule-1 (MAdCAM-1), which is mainly expressed on GALT and intestinal lamina propria (2–4). α4β7 has been proposed to play an important role in contributing to the pathogenesis of HIV by interacting with gp120 and assisting with the attachment of HIV to CD4+ T cells to promote the formation of synapses between virus and cells (5). Notably, a subset of CD4+ T cells expressing high levels of α4β7 is highly susceptible to HIV-1 infection (6), and availability of α4β7+ memory CD4+ T cells correlates with HIV acquisition and pathogenesis (7, 8). Moreover, α4β7+ memory CD4+ T cells are preferentially infected during early and acute HIV infection (9), and studies have shown that the administration of an anti-α4β7 monoclonal antibody (α4β7 mAb) at a dose of 50 mg/kg just before and during repeated low-dose challenges in rhesus macaques prevented or delayed vaginal simian immunodeficiency virus (SIV)/simian-human immunodeficiency virus (SHIV) infection and protected the GALT (10–12). These findings suggest that α4β7 could be targeted in the female genital mucosa to develop new strategies for the prevention of HIV vaginal transmission.

Notably, Entyvio (vedolizumab), a commercially available humanized mAb approved by the Food and Drug Administration (FDA) for the treatment of inflammatory bowel disease (IBD), has the same antigen-binding region as the anti-α4β7 antibody (13). Vedolizumab was shown to decrease lymphoid aggregates in HIV+ patients with IBD (14). Although one clinical trial reported that vedolizumab did not increase the time to viral rebound after analytical treatment interruption in HIV+ patients (15), preliminary data from a different trial (NCT03577782) suggest that it may have an impact on HIV rebound kinetics (McGiunty, Cameron, CROI 2019). As a mAb, this medication has to be administered intravenously and closely monitored during infusion. Adverse effects may occur including common flu-like symptoms (headache, sore throat, nasal congestion, sneezing, chills, fever, body pain, and tiredness), skin rash, gastrointestinal upset, and other rare effects like anaphylaxis and elevation of hepatic enzymes (16). The invasive administration route and the potential for systemic adverse effects of vedolizumab prompted our group to develop new formulations for vaginal delivery of the anti-α4β7 mAb as an HIV prophylaxis.

Nanoparticles (NPs) have small sizes within the range of 1 to 500 nm (17), allowing NPs to target the site of treatment more efficiently, thus enhancing local drug concentration while reducing systemic side effects (18). The larger surface area of NPs enables them to be modified with various functional molecules, including polymers, antibodies, aptamers, and proteins/peptides (18). These surface modifications endow NPs with additional beneficial properties such as cell targeting (18) and mucus penetration (19), facilitating further improvement in therapeutic efficacy. A wide range of novel intravaginal NP formulations have been developed to promote the delivery of small molecules (20), proteins/peptides (21), antigens (22), and nucleic acids (23) to prevent sexually transmitted infections including HIV, human papillomavirus, herpes simplex virus, and chlamydia trachomatis. Antibody- or antigen-conjugated NPs have gained increased attention in intravaginal drug delivery because of their abilities in facilitating targeted drug delivery (24), in induction of vaginal immunity (22), and as a diagnostic tool for vaginal infections (25). Intravaginal delivery of free antibodies has been a challenge because antibodies can tightly bind to cervicovaginal mucus (26), resulting in inefficient delivery to the target site. As a result, using NPs as a delivery vehicle for antibodies may be an option to overcome these obstacles.

[1]School of Pharmacy, University of Waterloo, 10 Victoria St. S A, Kitchener, Ontario N2G 1C5, Canada. [2]Center for Biomedical Research, Population Council, One Dag Hammarskjold Plaza, New York, NY 10017, USA. [3]Tulane National Primate Research Center, Tulane University, 6823 St. Charles Ave., New Orleans, LA 70118, USA. [4]Aaron Diamond AIDS Research Center, Rockefeller University, 455 1st Avenue #7, New York, NY 10016, USA.
*Corresponding author. Email: emmanuel.ho@uwaterloo.ca (E.A.H.); emartinelli@popcouncil.org (E.M.)
†These authors contributed equally to this work.

Poly(lactic-co-glycolic acid) (PLGA) is the most extensively used polymer for the development of intravaginal NP formulations. PLGA is an FDA-approved polymer and has many attractive properties, including biodegradability, biocompatibility, and versatility for encapsulating small and large molecules, achieving sustained drug release and surface modifications (27). Polyethylene glycol (PEG) is also an FDA-approved polymer, and its applications have been seen in many of the FDA-approved medications, including intravenous injections and liposomal formulations (28, 29). PEG in intravaginal formulations has been shown to improve the penetration of polymeric NPs through cervicovaginal mucus (19). Polyethylenimine (PEI) is a cationic polymer that has been widely studied for its applications in gene delivery (24), NP preparation (30), and surface coating (31). It has also been approved by the FDA for clinical use in pharmaceuticals and medical devices (32).

Gels prepared with bioadhesive polymers can adhere to tissues for prolonged durations compared with nonadhesive liquid preparations and increase the exposure period of tissues to active ingredients in gels (33). They have been widely used as intravaginal drug delivery systems for therapeutic proteins/peptides (34), antigens (35), and NPs (36). Hydroxyethylcellulose (HEC) is an FDA-approved polymer that is widely used in pharmaceutical manufacturing. Gels made from HEC are transparent, nonirritating, pharmacologically inactive, and compatible with a wide variety of therapeutic ingredients (37).

Herein, we describe the development and in vitro, ex vivo, and in vivo evaluation of a novel vaginal gel consisting of anti-$\alpha_4\beta_7$ mAb–conjugated NPs (NP-$\alpha_4\beta_7$ gel) for the delivery of therapeutic antibodies into the vaginal mucosa as a potential strategy for preventing vaginal transmission of HIV-1. The NP system is composed of PEI and PLGA-PEG prepared by a double emulsion (w/o/w) evaporation method. The anti-$\alpha_4\beta_7$ mAb is covalently conjugated on the surface of the NP by forming a covalent bond between the amine group of the antibody and the carboxyl group of the PLGA-PEG through chemical conjugation. Afterward, the NP-$\alpha_4\beta_7$ is loaded into a 1% HEC gel to prolong the contact time of NP-$\alpha_4\beta_7$ with the intravaginal lumen and provide ease in self-administration of the NPs. The NP-$\alpha_4\beta_7$ has optimal particle size and surface charge properties for mucus penetration and can efficiently block $\alpha_4\beta_7$ on immune cells in vitro and ex vivo. When intravaginally administered as a single dose in a rhesus macaque model, the formulation preferentially bound to CD4$^+$ or CD3$^+$ T cells expressing high levels of $\alpha_4\beta_7$. Blocking of the $\alpha_4\beta_7$ was restricted to the vaginal tract without any changes detected systemically.

## RESULTS

### Particle size and zeta potential
Previous studies have reported that the vaginal pH in macaques is ~6.0 to 7.0 because of lack of dominant lactobacilli in the microbio-ta, while the human vaginal pH is ~3.2 to 5.0 because of the massive presence of lactobacilli (38). Therefore, the NPs were characterized in two different types of medium: NaH$_2$PO$_4$ (pH 7.0) or vaginal fluid simulant (VFS; pH 4.2), to mimic the vaginal environment of macaques and humans, respectively. The average particle size for NP-$\alpha_4\beta_7$ was found to be within the range of 200 to 300 nm (Table 1). In neutral solution mimicking the vaginal environment of macaques, the average NP size was smaller in comparison to NPs suspended in VFS (pH 4.2). Zeta potential was also influenced by the medium the NPs were measured in. Acidic pH contributed to slightly higher zeta potential (1.68 ± 0.20 mV) compared with neutral pH (−0.01 ± 0.03 mV), but the zeta potentials in both medium were measured to be close to neutral for NP-$\alpha_4\beta_7$.

### Antibody conjugation efficiency and antibody loading
Antibody conjugation efficiency and concentration of antibody loading onto the NPs are shown in Table 2. Three different concentrations of $\alpha_4\beta_7$ antibody (0.7, 1.4, and 3.4 mg/ml) were evaluated during the formulation optimization process. The data showed that the antibody conjugation efficiency decreased as the input concentrations of $\alpha_4\beta_7$ antibody increased, resulting in an antibody conjugation efficiency of 45.7 ± 1.1%, 32.6 ± 0.5%, and 12.3 ± 0.2%, respectively. However, the antibody loading onto the NPs (µg Ab/mg NPs) increased as the input concentrations of $\alpha_4\beta_7$ antibody increased, with a maximum loading capacity of 43.4 ± 0.7 µg Ab/mg NPs achieved at 1.4 mg/ml. Further increase in $\alpha_4\beta_7$ antibody concentrations beyond 1.4 mg/ml did not further promote antibody loading onto the NPs. As a result, 1.4 mg/ml of $\alpha_4\beta_7$ antibody was the optimal conjugation concentration to achieve the highest antibody loading onto the NPs.

### In vitro NP-$\alpha_4\beta_7$ gel cell-binding studies
Next, we evaluated whether conjugating antibody to NPs and loading NP-$\alpha_4\beta_7$ into 1% HEC gel would affect the binding affinity of the antibody. An in vitro study comparing the antibody binding efficiency of free antibody and anti-$\alpha_4\beta_7$ mAb–conjugated NPs loaded in 1% HEC gel was conducted using RPMI 8866, a human lymphoblastoid cell line expressing high levels of $\alpha_4\beta_7$. To detect the antibody bound onto the surface of RPMI 8866 cells, phycoerythrin (PE)–labeled anti-$\alpha_4\beta_7$ mAb was conjugated to NPs during preparation. Cells treated with phosphate-buffered saline (PBS) and NP–immunoglobulin G (IgG) gel were used as control groups (Fig. 1, A and B). Formulations of NP-$\alpha_4\beta_7$ with two different antibody loadings (30.5 µg Ab/mg NPs and 43.4 µg Ab/mg NPs) were used to treat cells at the same concentration, resulting in corresponding PE$^+$ anti-$\alpha_4\beta_7$ antibody concentrations of 1.2 and 1.8 µg/ml, respectively. Because PE$^+$ anti-$\alpha_4\beta_7$ antibody accounts for 2% of the total antibody conjugated to NPs, the total antibody concentrations were about 60 and 90 µg/ml in the above treatment groups. Cells

Table 1. Particle size and zeta potential in different media. Values represent means ± SD, $n$ = 3.

| | NaH$_2$PO$_4$, pH 7.0 | | | VFS, pH4.2 | | |
| | Size (nm) | PDI | Zeta potential (mV) | Size (nm) | PDI | Zeta potential (mV) |
|---|---|---|---|---|---|---|
| NPs | 231.6 ± 15.0 | 0.254 | −7.29 ± 1.87 | 232.8 ± 6.8 | 0.247 | 1.22 ± 1.14 |
| NPs-$\alpha_4\beta_7$ Ab | 250.9 ± 3.0 | 0.328 | −0.01 ± 0.03 | 262.5 ± 4.0 | 0.167 | 1.68 ± 0.20 |

**Table 2. Antibody conjugation efficiency and antibody loading.** Values represent means ± SD, $n = 3$.

| Concentration of $\alpha_4\beta_7$ Ab (mg/ml) | Ab conjugation efficiency | Ab loading (µg Ab/mg NPs) |
|---|---|---|
| 0.7 | 45.7 ± 1.1% | 30.5 ± 0.7 |
| 1.4 | 32.6 ± 0.5% | 43.4 ± 0.7 |
| 3.4 | 12.3 ± 0.2% | 41.1 ± 0.7 |

were incubated with formulations for 2 and 24 hours and analyzed immediately for antibody binding efficiency. Results showed that after 2 hours of incubation, more than 85% (mean ± SD, 87.0 ± 1.5%) of cells were detected to be PE$^+$ in the group dosed with the low antibody loading formulation (Fig. 1C). After 24 hours of incubation, more than 90% (mean ± SD, 92.6 ± 1.5%) of cells were PE$^+$ (Fig. 1E), reaching similar levels as the group incubated with free antibody (Fig. 1G). Similar results also appeared in the group treated with the high antibody loading formulation, but maximum binding could be achieved as early as 2 hours (mean ± SD, 92.3 ± 0.9%) (Fig. 1D), and this effect was maintained until the 24-hour time point (mean ± SD, 92.2 ± 1.7%) (Fig. 1F).

## Ex vivo blockage of $\alpha_4\beta_7$ on cells in vaginal explants by NP-$\alpha_4\beta_7$ gel

After confirming the in vitro binding affinity of $\alpha_4\beta_7$-NP gel, we evaluated the formulation in an ex vivo polarized macaque vaginal explant model (39). Formulation with the same antibody loading (43.4 µg Ab/mg NPs) was used to dose vaginal explant tissues at two different antibody treatment concentrations (0.3 and 1.5 mg/ml) to compare the blockage of $\alpha_4\beta_7$. After 1 hour of incubation, the explant was washed and digested into a single-cell suspension. The cell suspension was stained with PE-labeled anti-$\alpha_4\beta_7$ mAb to identify $\alpha_4\beta_7$ that was not blocked by the formulation. A previous validation experiment demonstrated that the washing and digestion steps did not alter the binding of $\alpha_4\beta_7$ antibody and NP-$\alpha_4\beta_7$ to the $\alpha_4\beta_7$-expressing RPMI 8866 cell line. Compared with NP-IgG gel, the NP-$\alpha_4\beta_7$ gel could block more than 75% ($P = 0.0007$) of $\alpha_4\beta_7$ on CD4$^+$ T cells at an antibody treatment concentration of 1.5 mg/ml after only 1 hour of incubation, while the blockage efficiency at an antibody treatment concentration of 0.3 mg/ml was slightly lower at ~65% ($P = 0.0013$) (Fig. 2).

## In vivo blockage of $\alpha_4\beta_7$ in macaques after treatment with NP-$\alpha_4\beta_7$ gel

Last, we evaluated the in vivo blocking ability of NP-$\alpha_4\beta_7$ gel after a single intravaginal administration of the formulation in a rhesus macaque model. Baseline blood, vaginal, rectal, inguinal lymph node, and ectocervix biopsies were collected before and after the treatment (Fig. 3). Six macaques were treated with the NP-$\alpha_4\beta_7$ gel, and four were treated with a control NP-IgG gel. Baseline samples from one NP-$\alpha_4\beta_7$ gel–treated animal were lost, so the data from this animal were excluded from the analysis. Because the expression level of $\alpha_4\beta_7$ varies within each individual animal, the results were normalized to pre-NP gel administration levels. We primarily focused on the blockage of $\alpha_4\beta_7$ on T cells from vaginal tissue. However, the potential distal effect at other anatomical sites including peripheral blood mononuclear cells (PBMCs), rectum, inguinal
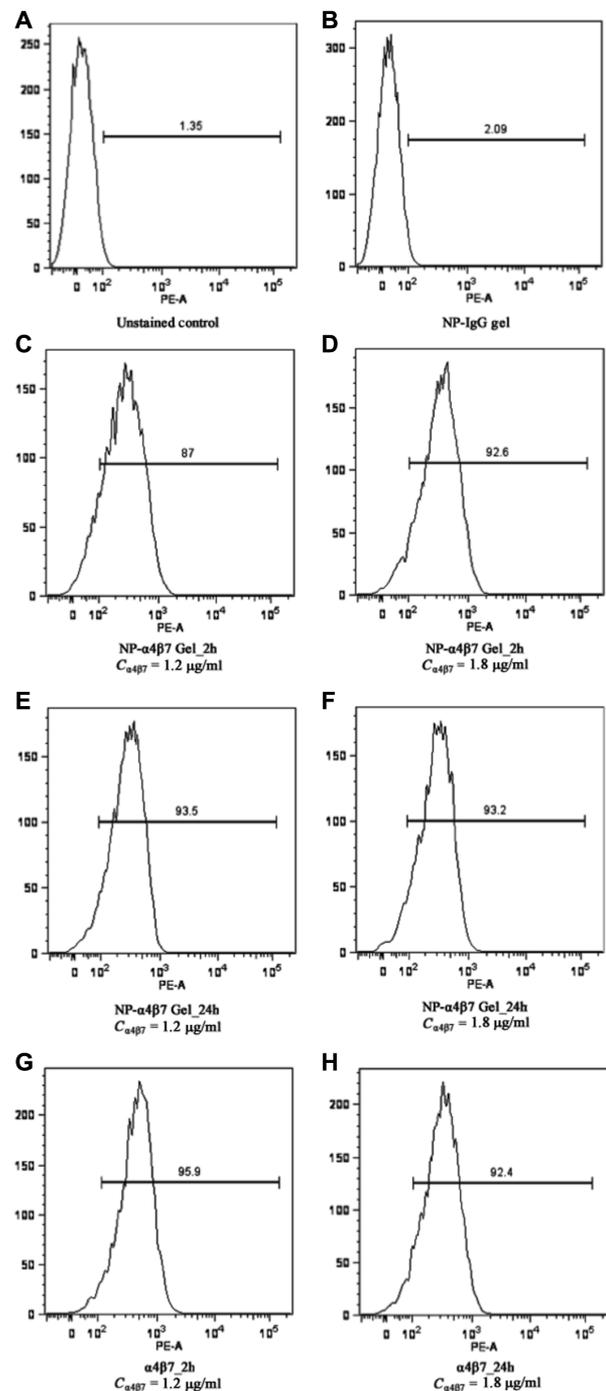


**Fig. 1. In vitro cell-binding study with NP-$\alpha_4\beta_7$ gel.** One-percent HEC gel loaded with 30.5 or 43.4 µg Ab/mg NPs (NP-$\alpha_4\beta_7$ gel) was used to treat cells for 2 and 24 hours. The $C_{\alpha_4\beta_7}$ shown in the graph represents the concentration of PE$^+$ anti-$\alpha_4\beta_7$ antibody. The data show representative histograms from a measurement of $n = 3$. The Y axis represents the number of cells/events, and the X axis represents the fluorescence intensity. The number above the gating line represents the percentage of PE$^+$ RPMI 8866 cells in each histogram. (**A**) Unstained control. (**B**) cells treated with NP-IgG gel. (**C**) cells treated with NP-$\alpha_4\beta_7$ gel ($C = 1.2$ µg/ml) for 2 hours. (**D**) cells treated with NP-$\alpha_4\beta_7$ gel ($C = 1.8$ µg/ml) for 2 hours. (**E**) cells treated with NP-$\alpha_4\beta_7$ gel ($C = 1.2$ µg/ml) for 24 hours. (**F**) cells treated with NP-$\alpha_4\beta_7$ gel ($C = 1.8$ µg/ml) for 24 hours. (**G**) cells treated with $\alpha_4\beta_7$ Ab ($C = 1.2$ µg/ml) for 2 hours. (**H**) cells treated with $\alpha_4\beta_7$ Ab ($C = 1.8$ µg/ml) for 24 hours. C, the concentration of PE$^+$ $\alpha_4\beta_7$ Ab.
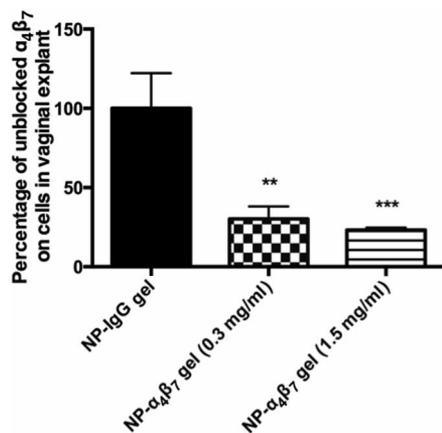
**Fig. 2. Ex vivo blockage of $\alpha_4\beta_7$ on CD4$^+$ T cells in rhesus macaque vaginal explants by NP-$\alpha_4\beta_7$ gel at two different antibody concentrations (0.3 and 1.5 mg/ml).** The graph shows the percentage of unblocked $\alpha_4\beta_7$ on cells in vaginal explant, quantified by staining the unblocked $\alpha_4\beta_7$ with PE$^+$ anti-$\alpha_4\beta_7$ antibody. One-percent HEC gel loaded with 43.4 µg Ab/mg NPs (NP-$\alpha_4\beta_7$ gel) was used for treatment. One-percent HEC gel loaded with 43.4 µg Ab/mg NPs (NP-IgG gel) was used as a control. The mean fluorescence intensity of PE$^+$ anti-$\alpha_4\beta_7$ antibody for each treatment group was normalized to the control group. Values represent means ± SD, $n = 4$. ***$P < 0.001$ and **$P < 0.01$ compared with NP-IgG gel.
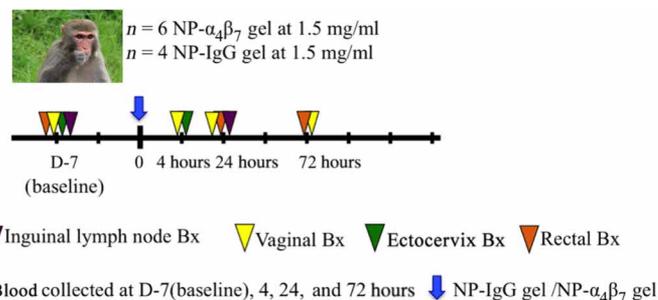


**Fig. 3. Schematic illustration of the treatment and sampling schedule for rhesus macaques.** D, day; Bx, biopsy. Photo credit: the photo "Rhesus macaques—Lion Hill, Hong Kong" was taken by cattan2011, acquired from Creative Commons, licensed under CC BY2.0 (free to share and adapt for any purpose, even commercially), and used without any modification. Photo link: https://ccsearch.creativecommons.org/photos/b4e1870b-7d54-485a-81d4-3c9e0fbc2137; license link: https://creativecommons.org/licenses/by/2.0/?ref=ccsearch&atype=rich.

lymph nodes, and ectocervix was explored to evaluate if the antibody was distributed systemically. Two-way analysis of variance (ANOVA) was used for data analysis (details explained below). On the basis of the vaginal tissue results (Fig. 4, A to D), there was statistical significance between NP-$\alpha_4\beta_7$ gel– and NP-IgG gel–treated groups in terms of $\alpha_4\beta_7$ blockage on memory $\alpha_4\beta_7$$^{high}$ CD4$^+$ T cells ($P = 0.0013$), total $\alpha_4\beta_7$$^+$ CD4$^+$ T cells ($P = 0.0006$), $\alpha_4\beta_7$$^{high}$ CD3$^+$ T cells ($P = 0.0004$), and total $\alpha_4\beta_7$$^+$ CD3$^+$ T cells ($P < 0.0001$). When compared with the baseline level, NP-IgG gel did not show any $\alpha_4\beta_7$ blockage effect, while the NP-$\alpha_4\beta_7$ gel decreased approximately 40% of $\alpha_4\beta_7$ on $\alpha_4\beta_7$$^{high}$ CD4$^+$ T cells 4 hours after administration ($P = 0.0187$) (Fig. 4A), and the effect lasted for 24 hours after treatment ($P = 0.0184$) and similar effects were seen in $\alpha_4\beta_7$$^{high}$ CD3$^+$ T cells as well ($P = 0.0112$ for 4 hours and $P = 0.0468$ for 24 hours) (Fig. 4C). Around 25% reduction in $\alpha_4\beta_7$ on total $\alpha_4\beta_7$$^+$ CD4$^+$ T cells was also observed in the NP-$\alpha_4\beta_7$ gel–treated group 24 hours after treatment ($P = 0.0117$) (Fig. 4B). Longer-lasting blockage effects of $\alpha_4\beta_7$ generated by NP-$\alpha_4\beta_7$ gel were observed in total $\alpha_4\beta_7$$^+$ CD3$^+$ T cells, as a significant reduction in $\alpha_4\beta_7$ (~23%) was maintained until 72 hours after treatment ($P = 0.0111$ for 4 hours, $P = 0.0016$ for 24 hours, and $P = 0.0015$ for 72 hours) (Fig. 4D). When we expanded the population of cells to $\alpha_4$$^+$ CD4$^+$ T cells and $\alpha_4$$^+$ CD3$^+$ T cells, the blockage effects were not seen (Fig. 4, E and F). As a result, the NP-$\alpha_4\beta_7$ gel specifically masked the $\alpha_4\beta_7$ on CD4$^+$ or CD3$^+$ T cells. Minor reductions in $\alpha_4\beta_7$ were observed in $\alpha_4\beta_7$$^{high}$ CD4$^+$ T cells and $\alpha_4\beta_7$$^+$ CD4$^+$ T cells in PBMC 4 hours after treatment with NP-$\alpha_4\beta_7$ gel; however, similar reduction trends were also seen in the group of animals treated with NP-IgG gel (Fig. 4, G and H). Therefore, it is likely that these changes were because of the fluctuation of $\alpha_4\beta_7$ expression level rather than the blockage effect of NP-$\alpha_4\beta_7$ gel. The $\alpha_4\beta_7$ blockage effect of the NP gel formulation was restricted to the vaginal tissues because no significant decrease in the levels of $\alpha_4\beta_7$ in CD4$^+$ T cells and/or CD3$^+$ T cells was detected in rectal tissue (Fig. 4, I and J), inguinal lymph nodes (Fig. 4, K and L), or ectocervix (Fig. 4, M to P).

## DISCUSSION

The female genital tract consists of a complex environment that can affect intravaginal drug delivery (40). The vaginal tract is covered by a thin layer of mucus that serves as a barrier to trap external invading pathogens, while also limiting drug penetration (40). The cervicovaginal mucus is composed of 95% water, 2% to 5% mucin fibers, and trace amounts of lactic acid, lipids, salts, proteins, enzymes, and cells (41). Mucin fibers, the main component, are large molecules formed by the linking of numerous mucin monomers (42, 43). They are negatively charged due to the presence of carboxyl or sulfate groups on mucin proteoglycans (44). Disulfide bond–stabilized globular regions are also present along mucin fibers, which contributes to their hydrophobicity nature (44). Mucin fibers cross-link into tiny nets in which water is trapped, forming thousands of microscale watery channels (19, 45). The physical contacts between drug molecules/drug vectors and mucin fibers generate multiple adhesive interactions, including physical entanglement, hydrophobic interaction, and electrostatic attraction (46). As a result, compounds or systems having a too small or too large size (as discussed in details below), are hydrophobic in nature, or having a positive-charged surface will be notably trapped in cervicovaginal mucus.

Even though the mesh pore size of the mucin network is 3 to 10 µm, the size of particles that can penetrate mucus is much smaller than that (46). It has been reported that the optimal size of nonadhesive particles for mucus penetration is 200 to 500 nm (46). Larger particles (>500 nm) are trapped in the apical layer of the vagina, while smaller particles (<200 nm) are trapped within the deeper layers of the vagina due to "dead-end" channels within the mucin network (46). Adhesive particles are largely trapped in the mucus regardless of size (46). The functionalization of NPs with low molecular weight (MW), hydrophilic polymer, and PEG (MW, ~2000) has been used to fabricate nonadhesive particles (19). Therefore, in our study, we used PLGA-PEG (10,000–2000) to fabricate NP with optimal size (~250 nm), close to neutral surface charge (zeta potential, ~0 mV), and is hydrophilic in nature (PEG on the surface) for enhanced mucus penetration and improved delivery of antibody to the epithelial layer in the vaginal mucosa.
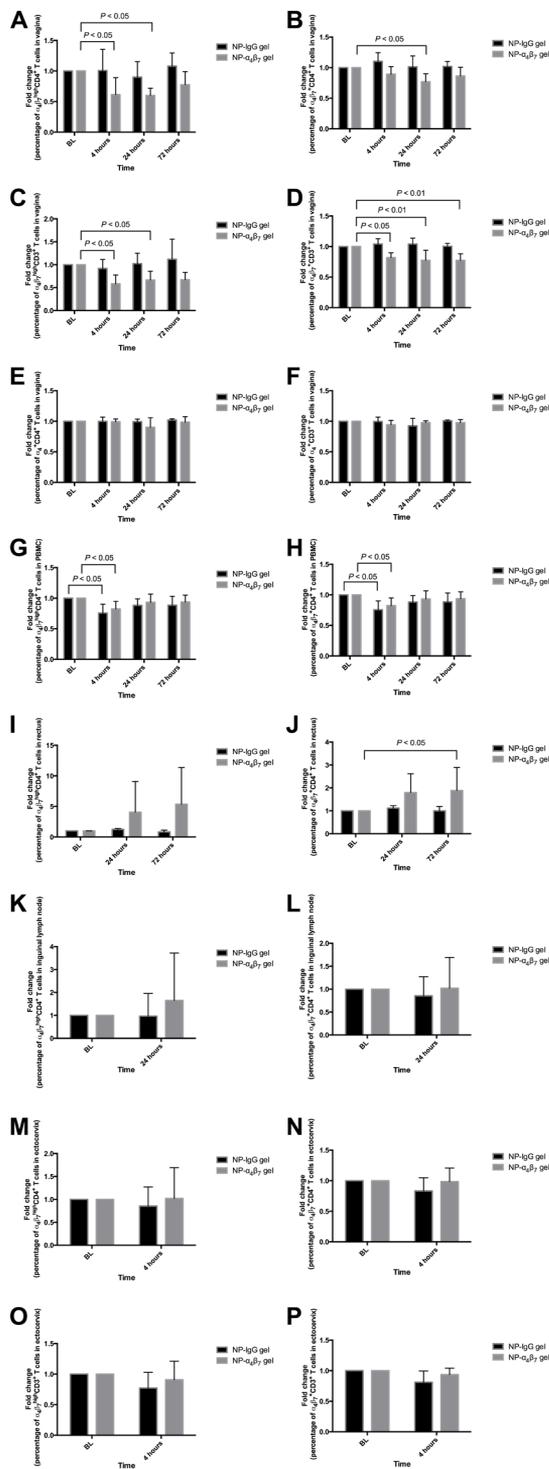
**Fig. 4. In vivo blockage of $\alpha_4\beta_7$ on tissues by NP-$\alpha_4\beta_7$ gel at an antibody concentration of 1.5 mg/ml in a rhesus macaque model.** One-percent HEC gel loaded with 43.4 μg Ab/mg NPs (NP-$\alpha_4\beta_7$ gel) was used for treatment. One-percent HEC gel loaded with 43.4 μg Ab/mg NPs (NP-IgG gel) was used as a control. BL, baseline. (**A** to **F**) Vagina, (**G** and **H**) PBMC, (**I** and **J**) rectus, (**K** and **L**) inguinal lymph nodes, (**M** to **P**) ectocervix. $P < 0.05$ or $P < 0.01$ compared with baseline. (A to P) $n = 4$ for NP-IgG gel–treated group, $n = 5$ for NP-$\alpha_4\beta_7$ gel–treated group (one of the rhesus macaques, IK06, was excluded because no cells were recovered at the time point of 0 for flow cytometry analysis).

Previous literature has indicated that PEI can be coated onto the surface of PLGA NPs through the cationic-anionic interaction between PEI and PLGA by incubating PLGA NPs in a certain concentration of PEI aqueous solution (31). Other literature have reported that PEI could form coatings onto the surface of PLGA–egg phosphatidylcholine NPs through electrostatic interaction when PEI is dissolved in the aqueous phase and PLGA–egg phosphatidylcholine is dissolved in the acetone-methanol phase for NP preparation through nanoprecipitation (47). In our system, we performed the opposite by dissolving PEI in the most inner aqueous phase ($w_1$) and the PLGA-PEG in the oil phase (o; methylene chloride). After the formation of a double emulsion ($w_1/o/w_2$) via sonication, PEI in the primary aqueous phase ($w_1$) will facilitate the electrostatic assembly of PEI (cationic)–PLGA (anionic) building block in the core of NPs. As the oil phase is evaporated off, PLGA is exposed to the primary aqueous phase. At the same time, the hydrophilic PEG end in PLGA-PEG polymer will align toward the secondary aqueous phase [$w_2$; polyvinyl alcohol (PVA) solution] forming PLGA-PEG NPs with the PLGA end facing the inner core and the PEG end facing the outer surface. This orderly alignment of PLGA-PEG will allow more PEG to be arranged on the surface to promote NP penetration through the cervicovaginal mucus for improved intraepithelial drug delivery.

Gel loaded with NPs has enhanced rheological properties; therefore, under certain shear stress, improvement to viscosity can be achieved with NP-loaded gel compared with the blank gel (20). With increased viscosity, prolonged residence time of NP-loaded gel would be expected when the gel is applied intravaginally. However, increased viscosity can act as a double-edged sword for the delivery of NPs. On the one hand, the increased viscosity can prolong direct contact between NPs and the vaginal compartment for enhanced drug delivery. On the other hand, increased viscosity may inhibit the release of NPs from the gel. As a result, the loading density of NPs into the gel and the concentration of polymer used for formulating the gel should be carefully designed and evaluated to achieve the optimal NP gel system.

Increased concentration of antibody enhanced the interaction between activated NPs and antibody, resulting in improved amounts of antibody conjugated onto the surface of NPs. However, as the concentration of antibody increased, the surface of NPs that could react with the antibody started to reach saturation, resulting in decreased conjugation efficiency. Here, we have shown that the conjugation of anti-$\alpha_4\beta_7$ antibody to NPs and formulation into a gel dosage form do not alter its binding efficiency to $\alpha_4\beta_7$ in comparison to free antibody as determined in vitro using RPMI 8866 cells expressing high levels of $\alpha_4\beta_7$. The percentage of PE+ cells did not reach 100% in either case probably because of a small percentage of the antibody being taken up into the cells. In the ex vivo vaginal explant model, greater than 75% of $\alpha_4\beta_7$ expressed on the cell surface was blocked by the NP-$\alpha_4\beta_7$ gel within 1 hour, indicating a rapid and efficient blocking ability of the conjugated antibody. The percentage of $\alpha_4\beta_7$ blocked on cells from vaginal explant tissue did not reach 100% possibly because (i) the incubation period was too short (1 hour) and no shear stress was present to help the gel formulation completely release all of the NPs, or (ii) the formulation has limited ability in blocking cells in explant tissues that express low levels of $\alpha_4\beta_7$, or (iii) the formulation could not completely penetrate into the tissues because of the tight junction of the intravaginal epithelium.

As a result, our next step was to evaluate the formulation in a nonhuman primate model. The NP-$\alpha_4\beta_7$ loaded in 1% HEC gel preferentially bound to T cells expressing high levels of $\alpha_4\beta_7$ in the vagina with significant blockage observed within 72 hours after administration of a single dose. It appears that penetration of NPs across vaginal tissue requires a few days to accomplish. The overall blockage of $\alpha_4\beta_7$ among intravaginal cells (high and low expression of $\alpha_4\beta_7$) was not as high as that of $\alpha_4\beta_7^{high}$ T cells, indicating a limited binding ability of the formulation to cells expressing a low level of $\alpha_4\beta_7$. Therefore, a multiple dosing regimen may be considered to achieve optimal receptor coverage. In addition, therapeutic efficacy may be improved in future formulations by using directional antibody conjugation (48–50). This orients the Fc region of the antibody to be conjugated to NPs, exposing the antigen-binding sites. This can be achieved by using specific chemical linkers between the antibody and NPs. Furthermore, directional antibody conjugation will increase homogeneity of synthesized NPs, maximize antigen-binding efficiency, minimize antigen-binding variations among different batches of NPs, and reduce dosing. All of this will improve the safety of NPs by minimizing adverse effects. Previous studies have shown that small interfering RNA (siRNA)–loaded PLGA NPs with a particle size of about 200 nm could penetrate approximately 75 μm into the intraepithelium of mouse vagina and achieve sustained gene knockdown (51). Our NPs blocked $\alpha_4\beta_7$ on the immune cells within the epithelium and, perhaps, even within the mucosal layer (vaginal biopsies include both epithelium and mucosa). Thus, we can conclude that our NP-$\alpha_4\beta_7$ successfully penetrated the epithelial layer. However, future studies should address the exact depth of penetration. In rhesus macaques, infusion of two doses of anti-$\alpha_4\beta_7$ mAb at 50 mg/kg resulted in more than 99% coverage of the $\alpha_4\beta_7$ on CD4$^+$ T cells in the cervicovaginal compartment (11). In comparison, the blocking efficiency is much lower with our NP-$\alpha_4\beta_7$. However, additional dosing and use of site-specific conjugation techniques may improve coverage. Ultimately, future work will need to determine the degree of $\alpha_4\beta_7$ blockade required for protection against HIV-1 vaginal infection. A major advantage of this topical formulation is that the $\alpha_4\beta_7$-blocking effects were restricted to the vaginal tract (e.g., the site of HIV transmission). In comparison to the intravenous formulation, this topical formulation should minimize systemic and off-target side effects, and this will need to be evaluated in the future. We observed fluctuations in the intravaginal $\alpha_4\beta_7$-blocking effects in macaques. This may possibly be attributed to two reasons. First, the in vivo study was performed under natural menstruation cycling (macaques were not injected with Depo-Provera). The thickness of the vaginal epithelium and the discharge of cervicovaginal fluid are significantly influenced by menstrual cycles (52, 53). As a result, different stages of the menstrual cycle may cause fluctuations of NP penetration ability into vaginal tissues. Second, different macaques may express significantly different levels of $\alpha_4\beta_7$ in vaginal tissues; therefore, those expressing low levels of $\alpha_4\beta_7$ may exhibit weaker blocking effects when treated with NP-$\alpha_4\beta_7$ gel. In the future, further in vivo studies could be proposed to address these points to get a better understanding of the therapeutic efficacy. For example, it would be interesting to determine whether intravaginal treatment of macaques with free $\alpha_4\beta_7$ antibody gel is effective in blocking $\alpha_4\beta_7$ on the surface of vaginal lymphocytes. Future studies should also evaluate the duration of the blocking effect and the safety profile, e.g., measuring the cytokine levels in the vaginal lumen.

In summary, the anti-$\alpha_4\beta_7$ mAb–conjugated NPs described here present a novel strategy to deliver the anti-$\alpha_4\beta_7$ antibody intravaginally. The ability to block integrin $\alpha_4\beta_7$ directly and exclusively on vaginal T cells may offer a new approach toward preventing the vaginal transmission of HIV-1 and suggests that NPs may be an effective way to deliver therapeutic antibodies that target molecules on the surface of immune cells.

## MATERIALS AND METHODS
### Ethics statement
Ten female Indian-origin rhesus macaques (*Macaca mulatta*; mean age, 8.3 years; range, 5.8 to 17 years; mean weight, 8.4 kg; range, 5.4 to 10.65 kg) were used in compliance with the regulations under the Animal Welfare Act, the *Guide for the Care and Use of Laboratory Animals*, at Tulane National Primate Research Center (TNPRC; Covington, LA). Animals were socially housed indoors in climate-controlled conditions with a 12/12-light/dark cycle.

All animals in this study were monitored twice daily to ensure proper welfare. Any abnormalities, including those related to appetite, stool, or behavior, were recorded and reported to a veterinarian. The animals were fed with commercially prepared macaque chow, twice daily. Supplemental food was provided in the form of fruit, vegetables, and foraging treats as part of the TNPRC environmental enrichment program. Water was available at all times through an automatic watering system. The TNPRC environmental enrichment program is reviewed and approved by the Institutional Animal Care and Use Committee semiannually. Veterinarians at the TNPRC Division of Veterinary Medicine have established procedures to minimize pain and distress through several means. Macaques were anesthetized with ketamine-HCl (10 mg/kg) or tiletamine/zolazepam (6 mg/kg) before all procedures. Preemptive and postprocedural analgesia (buprenorphine 0.01 mg/kg) was required for procedures that would likely cause more than momentary pain or distress in humans undergoing the same procedures. The above listed anesthetics and analgesics were used to minimize pain or distress associated with this study in accordance with the recommendations of the Weatherall Report. All studies were approved by the Animal Care and Use Committee of the TNPRC (OLAW assurance #A4499-01) and in compliance with animal care procedures. TNPRC is accredited by the Association for Assessment and Accreditation of Laboratory Animal Care (AAALAC #000594).

### Preparation of vaginal gel loading anti-$\alpha_4\beta_7$ mAb–conjugated NPs
NPs were fabricated with PEI (branched, MW 25K) (Sigma-Aldrich, Ontario, Canada) and PLGA-PEG (PLGA-PEG-COOH; 10K-2K) (Advanced Polymer Materials, Quebec, Canada) by a double emulsion evaporation method reported previously (51). In brief, 150 μl of tris-EDTA (ThermoFisher Scientific, Ontario, Canada) buffer was mixed with equal volume of PEI (0.372 mg/ml) followed by the addition of 600 μl of PLGA-PEG-COOH (10 mg/ml) (dissolved in methylene chloride, high-performance liquid chromatography grade, ThermoFisher Scientific, Ontario, Canada). The mixture was emulsified by sonication for 15 s, and the primary emulsion was combined with 4.3 ml of 2% PVA (MW, 31K-50K; Sigma-Aldrich, Ontario, Canada) and sonicated for another 2 min. The resulting emulsion was stirred at 4°C for more than 3 hours to evaporate the organic solvent and harden the particles. The NPs were collected by

centrifugation and washed with double-distilled water to remove excess PVA. Approximately, 6 mg of NPs was resuspended in 1.7 ml of 0.1 M 2-(N-morpholino) ethanesulfonic acid (Sigma-Aldrich, Ontario, Canada) buffer (pH 6.0), then 200 μl of 1-ethyl-3-(3-dimethylaminopropyl) carbodiimide (EDC; 200 mg/ml; G-Biosciences, Missouri, USA) and 100 μl of N-hydroxysuccinimide (NHS; 275 mg/ml; G-Biosciences, Missouri, USA) were added to the suspension. The mixture was stirred at room temperature for 1 hour to activate the carboxyl group, and then, the activated NPs were collected by centrifugation to remove excess EDC and NHS. The NPs were then resuspended in 0.1 M $NaH_2PO_4$ (ThermoFisher Scientific, Ontario, Canada) buffer (pH 7.4), and anti-$\alpha_4\beta_7$ mAb ($\alpha_4\beta_7$ Ab, MassBiologics, Massachusetts, USA) was added to the suspension, resulting in a final volume of 290 μl. Three different concentrations of $\alpha_4\beta_7$ Ab (0.7, 1.4, and 3.4 mg/ml) were evaluated for conjugation efficiency and antibody loading during the optimization stage. The mixture was stirred at room temperature for 4 hours to facilitate antibody conjugation. Antibody conjugation efficiency was measured by directly quantifying the antibody on NPs using the BCA kit (ThermoFisher Scientific, Ontario, Canada). Last, the NP-$\alpha_4\beta_7$ was separated from unconjugated antibody by centrifugation and formulated into a 1% HEC (250 HX Pharma, Ashland, Kentucky, USA) gel. Initially, a 2% HEC gel was prepared by dissolving HEC in 0.1 M $NaH_2PO_4$ buffer (pH 7.4), and the final pH was adjusted to 7.0. The resulting NP-$\alpha_4\beta_7$ was then resuspended in 0.1 M $NaH_2PO_4$ buffer (pH 7.0), and equal volumes of 2% HEC gel and NP-$\alpha_4\beta_7$ suspension were combined together and mixed to obtain a homogenous formulation of 1% HEC gel loaded with NP-$\alpha_4\beta_7$.

### Characterization of NP-$\alpha_4\beta_7$
For measuring particle size and zeta potential, NPs were resuspended in $NaH_2PO_4$ (pH 7.0) or VFS (pH 4.2) at a concentration of 25 μg/ml. Particle size was determined by dynamic light scattering (DLS) using ZetaPALS (Brookhaven Instruments, New York, USA). Zeta potential was also determined using DLS under Smoluchowski mode. Samples were analyzed in triplicate for three runs at 2 min each.

### In vitro NP-$\alpha_4\beta_7$ cell-binding studies
RPMI 8866, a human lymphoblastoid cell line expressing high levels of $\alpha_4\beta_7$, was purchased from Sigma-Aldrich (Ontario, Canada) and maintained in RPMI 1640 containing 2 mM glutamine (Corning, Ontario, Canada) supplemented with 10% fetal bovine serum (FBS; ThermoFisher Scientific, Ontario, Canada). PE-labeled anti-$\alpha_4\beta_7$ mAb (2% of the total antibody for conjugation) was used for cellular detection. NP-$\alpha_4\beta_7$ with an antibody loading of 30.5 and 43.4 μg Ab/mg NPs (as indicated in Table 2) was prepared and formulated into 1% HEC gel following the method mentioned above. On the day of the experiment, approximately $3 \times 10^5$ cells were seeded onto 24-well plates in 500 μl of culture medium per well. Cells were incubated with 1% HEC gel loaded with NP-$\alpha_4\beta_7$ containing two different antibody loadings for 2 and 24 hours. The final concentrations of PE-labeled anti-$\alpha_4\beta_7$ antibody in each group were about 1.2 and 1.8 μg/ml. Cells were collected and washed with cold PBS (ThermoFisher Scientific, Ontario, Canada) and analyzed using flow cytometry (Canto II, BD, Ontario, Canada) immediately to quantify the percentage of $PE^+$ cells.

### Ex vivo vaginal explant studies
Macaque vaginal tissue biopsy samples were collected using a biopsy punch (5 mm by 5 mm; two pieces; ThermoFisher Scientific, Massachusetts,

USA) and placed on ice in L15 medium (ThermoFisher Scientific, Massachusetts, USA) containing 10% FBS (ThermoFisher Scientific, Massachusetts, USA), penicillin (100 U/ml), and streptomycin (100 μg/ml) (ThermoFisher Scientific, Massachusetts, USA). Tissues were extensively washed with PBS and placed onto a 24-well Transwell insert (3-mm pore size; Corning, New York, USA) with the mucosa side facing up. The epithelium was surrounded with 3% agarose, and the basolateral chamber was filled with Dulbecco's modified Eagle's medium (ThermoFisher Scientific, Massachusetts, USA) supplemented with 10% FBS, penicillin (100 unit/ml), streptomycin (100 μg/ml), and nonessential amino acids. A dose of 20 or 100 μl of 1% HEC gel loaded with NP-$\alpha_4\beta_7$ (43.4 μg Ab/mg NPs) was added to the tissues, resulting in two different antibody concentrations (0.3 and 1.5 mg/ml). The tissues were incubated at 37°C, 5% $CO_2$ in a humidified incubator for 1 hour. At the end of treatment, tissues were removed from the insert and extensively washed with PBS. For digestion, the washed tissues were cut into small pieces in a small petri dish containing collagenase IV (Worthington Biochemical, New Jersey, USA), Hanks' balanced salt solution (HBSS) buffer (ThermoFisher Scientific, Massachusetts, USA) and incubated for 40 min at 37°C on a shaking platform. Digested tissues were then passed through a 40-micrometer cell strainer. Cell suspensions were stained with the viability dye LIVE/DEAD Aqua dye (Molecular Probes, Massachusetts, USA) before being incubated with a combination of anti-CD4 (H7), anti-CD3 (V450), and anti-$\alpha_4\beta_7$ (PE) antibodies from BD Biosciences (California, USA). Cells were incubated with the antibodies for 20 min at 4°C, washed, and fixed in 2% paraformaldehyde (BD Biosciences, California, USA). Samples were analyzed on a BD LSRII Flow Cytometer.

### Rhesus macaque $\alpha_4\beta_7$-blocking studies
For the in vivo study, 1% HEC gel loaded with NP-$\alpha_4\beta_7$ or NP-IgG (43.4 μg Ab/mg NPs) was used to dose the animals. Ten rhesus macaques were divided into two groups and administered intravaginally with either 3 ml of NP-$\alpha_4\beta_7$ gel ($C_{anti-\alpha4\beta7\ antibody}$ = 1.5 mg/ml; six animals) or 3 ml of NP-IgG gel ($C_{IgG\ antibody}$ = 1.5 mg/ml; four animals) after anesthesia administration (animals were anesthetized for 40 min for the procedure and to allow absorption). Samples were collected at baseline (7 days before treatment), 4, 24, and 72 hours after treatment as indicated in the sampling schematic (Fig. 3). Depot medroxyprogesterone acetate was not administered, and the menstrual cycle of these macaques was not monitored. Blood and various tissues, including inguinal lymph nodes and mucosal tissues (rectal, vaginal, and ectocervix), were collected.

Mucosal tissues were cut into small pieces and washed in HBSS with $Ca^{2+}/Mg^{2+}$ and digested for 45 min in HBSS supplemented with collagenase IV (1 mg/ml) and human serum albumin (1 mg/ml) (ThermoFisher Scientific, Massachusetts, USA) on a shaking platform at 37°C. Cell suspension was then passed through a 40-μm nylon cell strainer. Lymph nodes were cut into small pieces and passed directly through a 40-μm cell strainer. PBMCs were isolated using Ficoll-Hypaque density gradient centrifugation.

Cell suspensions were stained with the viability dye LIVE/DEAD Aqua dye (Molecular Probes, Massachusetts, USA) before being incubated with a combination of anti-CD4 (BUV395), anti-CD3 (V450), and anti-CD95 (PerCP-Fluor 710) antibodies from BD Biosciences (California, USA). Cells were also stained with anti-CD49d (integrin alpha 4, NovusBio) and anti-$\alpha_4\beta_7$ (PE, nonhuman primate repository, Beth Israel Medical Center, Massachusetts,

USA). Cells were incubated with the antibodies for 20 min at 4°C, washed, and fixed in 2% paraformaldehyde. Greater than 200,000 events were acquired in the lymphocyte live cell gate using the BD LSRII Flow Cytometer. Data were analyzed with FlowJo 9.9.4.

## Statistical analysis

One-way ANOVA test was used to compare the statistical significance between NP-IgG gel and NP-α₄β₇ Ab gel in the ex vivo study (Fig. 2), α = 0.05. Two-way ANOVA test was used to compare the statistical significance between NP-IgG gel and NP-α₄β₇ Ab gel in the in vivo study (Fig. 4), α = 0.05. Tabular results and Dunnett's multicomparison results were reported.

## REFERENCES AND NOTES

1. M. Barczyk, S. Carracedo, D. Gullberg, Integrins. *Cell Tissue Res.* **339**, 269–280 (2010).
2. A. Petrovic, O. Alpdogan, L. M. Willis, J. M. Eng, A. S. Greenberg, B. J. Kappel, C. Liu, G. J. Murphy, G. Heller, M. R. M. van den Brink, LPAM (α₄β₇ integrin) is an important homing integrin on alloreactive T cells in the development of intestinal graft-versus-host disease. *Blood* **103**, 1542–1547 (2004).
3. C. Berlin, R. F. Bargatze, J. J. Campbell, U. H. von Andrian, M. C. Szabo, S. R. Hasslen, R. D. Nelson, E. L. Berg, S. L. Erlandsen, E. C. Butcher, α4 integrins mediate lymphocyte attachment and rolling under physiologic flow. *Cell* **80**, 413–422 (1995).
4. E. C. Butcher, L. J. Picker, Lymphocyte homing and homeostasis. *Science* **272**, 60–66 (1996).
5. J. Arthos, C. Cicala, E. Martinelli, K. Macleod, D. V. Ryk, D. Wei, Z. Xiao, T. D. Veenstra, T. P. Conrad, R. A. Lempicki, S. McLaughlin, M. Pascuccio, R. Gopaul, J. McNally, C. C. Cruz, N. Censoplano, E. Chung, K. N. Reitano, S. Kottilil, D. J. Goode, A. S. Fauci, HIV-1 envelope protein binds to and signals through integrin α₄β₇, the gut mucosal homing receptor for peripheral T cells. *Nat. Immunol.* **9**, 301–309 (2008).
6. C. Cicala, E. Martinelli, J. P. McNally, D. J. Goode, R. Gopaul, J. Hiatt, K. Jelicic, S. Kottilil, K. Macleod, A. O'Shea, N. Patel, D. V. Ryk, D. Wei, M. Pascuccio, L. Yi, L. McKinnon, P. Izulla, J. Kimani, R. Kaul, A. S. Fauci, J. Arthos, The integrin α₄β₇ forms a complex with cell-surface CD4 and defines a T-cell subset that is highly susceptible to infection by HIV-1. *Proc. Natl. Acad. Sci. U.S.A.* **106**, 20877–20882 (2009).
7. E. Martinelli, F. Veglia, D. Goode, N. Guerra-Perez, M. Aravantinou, J. Arthos, M. Piatak Jr., J. D. Lifson, J. Blanchard, A. Gettie, M. Robbiani, The frequency of α₄β₇^high memory CD4⁺ T cells correlates with susceptibility to rectal simian immunodeficiency virus infection. *J. Acquir. Immune. Defic. Syndr.* **64**, 325–331 (2013).
8. A. Sivro, A. Schuetz, D. Sheward, V. Joag, S. Yegorov, L. J. Liebenberg, N. Yende-Zuma, A. Stalker, R. S. Mwatelah, P. Selhorst, N. Garrett, N. Samsunder, A. Balgobin, F. Nawaz, C. Cicala, J. Arthos, A. S. Fauci, A. O. Anzala, J. Kimani, B. S. Bagaya, N. Kiwanuka, C. Williamson, R. Kaul, J.-A. S. Passmore, N. Phanuphak, J. Ananworanich, A. Ansari, Q. A. Karim, S. S. A. Karim, L. R. McKinnon; CAPRISA, RV study groups, Integrin α₄β₇ expression on peripheral blood CD4⁺ T cells predicts HIV acquisition and disease progression outcomes. *Sci. Transl. Med.* **10**, eaam6354 (2018).
9. A. Tokarev, L. R. McKinnon, A. Pagliuzza, A. Sivro, T. E. Omole, A. Kroon, N. Chomchey, N. Phanuphak, A. Schuetz, M. L. Robb, M. A. Eller, J. Ananworanich, N. Chomont, D. L. Bolton, Preferential infection of α4β7⁺ memory CD4⁺ T cells during early acute HIV-1 infection. *Clin. Infect. Dis.* , ciaa497 (2020).
10. S. N. Byrareddy, B. Kallam, J. Arthos, C. Cicala, F. Nawaz, J. Hiatt, E. N. Kersh, J. M. McNicholl, D. Hanson, K. A. Reimann, M. Brameier, L. Walter, K. Rogers, A. E. Mayne, P. Dunbar, T. Villinger, D. Little, T. G. Parslow, P. J. Santangelo, F. Villinger, A. S. Fauci, A. A. Ansari, Targeting α₄β₇ integrin reduces mucosal transmission of simian immunodeficiency virus and protects gut-associated lymphoid tissue from infection. *Nat. Med.* **20**, 1397–1400 (2014).
11. L. E. Pereira, N. Onlamoon, X. Wang, R. Wang, J. Li, K. A. Reimann, F. Villinger, K. Pattanapanyasat, K. Mori, A. A. Ansari, Preliminary *in vivo* efficacy studies of a recombinant rhesus anti-α₄β₇ monoclonal antibody. *Cell. Immunol.* **259**, 165–176 (2009).
12. G. Calenda, I. Frank, G. Arrode-Brusés, A. Pegu, K. Wang, J. Arthos, C. Cicala, K. A. Rogers, L. Shirreff, B. Grasperge, J. L. Blanchard, S. Maldonado, K. Roberts, A. Gettie, F. Villinger, A. S. Fauci, J. R. Mascola, E. Martinelli, Delayed vaginal SHIV infection in VRC01 and anti-α4β7 treated rhesus macaques. *PLOS Pathog.* **15**, e1007776 (2019).
13. C. V. Kemseke, E. Louis, C. Reenaers, Vedolizumab (Entyvio®) for the treatment of inflammatory bowel diseases. *Rev. Med. Liege* **70**, 575–582 (2015).
14. M. Uzzan, M. Tokuyama, A. K. Rosenstein, C. Tomescu, I. N. SahBandar, H. M. Ko, L. Leyre, A. Chokola, E. Kaplan-Lewis, G. Rodriguez, A. Seki, M. J. Corley, J. Aberg, A. L. Porte,
15. E.-Y. Park, H. Ueno, I. Oikonomou, I. Doron, I. D. Iliev, B. K. Chen, J. Lui, T. W. Schacker, G. C. Furtado, S. A. Lira, J.-F. Colombel, A. Horowitz, J. K. Lim, N. Chomont, A. H. Rahman, L. C. Montaner, L. C. Ndhlovu, S. Mehandru, Anti-α4β7 therapy targets lymphoid aggregates in the gastrointestinal tract of HIV-1–infected individuals. *Sci. Transl. Med.* **10**, eaau4711 (2018).
15. M. C. Sneller, K. E. Clarridge, C. Seamon, V. Shi, M. D. Zorawski, J. S. Justement, J. Blazkova, E. D. Huiting, M. A. Proschan, J. R. Mora, M. Shetzline, S. Moir, H. C. Lane, T.-W. Chun, A. S. Fauci, An open-label phase 1 clinical trial of the anti-α₄β₇ monoclonal antibody vedolizumab in HIV-infected individuals. *Sci. Transl. Med.* **11**, eaax3447 (2019).
16. H. Singh, N. Grewal, E. Arora, H. Kumar, A. K. Kakkar, Vedolizumab: A novel anti-integrin drug for treatment of inflammatory bowel disease. *J. Nat. Sci. Biol. Med.* **7**, 4–9 (2016).
17. C. Wilson, A. Magnaudeix, C. Naves, F. Vincent, F. Lalloue, M.-O. Jauberteau, The ins and outs of nanoparticle technology in neurodegenerative diseases and cancer. *Curr. Drug Metab.* **16**, 609–632 (2015).
18. R. Singh, J. W. Lillard, Nanoparticle-based targeted drug delivery. *Exp. Mol. Pathol.* **86**, 215–223 (2009).
19. S. K. Lai, Y.-Y. Wang, J. Hanes, Mucus-penetrating nanoparticles for drug and gene delivery to mucosal tissues. *Adv. Drug Deliv. Rev.* **61**, 158–171 (2008).
20. S. Yang, Y. Chen, K. Gu, A. Dash, C. L. Sayre, N. M. Davies, E. A. Ho, Novel intravaginal nanomedicine for the targeted delivery of saquinavir to CD4⁺ immune cells. *Int. J. Nanomedicine* **8**, 2847–2858 (2013).
21. T. Kawamura, S. E. Bruse, A. Abraha, M. Sugaya, O. Hartley, R. E. Offord, E. J. Arts, P. A. Zimmerman, A. Blauvelt, S. E. Bruce, PSC-RANTES blocks R5 human immunodeficiency virus infection of langerhans cells isolated from individuals with a variety of CCR5 diplotypes. *J. Virol.* **78**, 7602–7609 (2004).
22. G. Galliverti, M. Tichet, S. Domingos-Pereira, S. Hauert, D. Nardelli-Haefliger, M. A. Swartz, D. Hanahan, S. Wullschleger, Nanoparticle conjugation of human papillomavirus 16 E7-long peptides enhances therapeutic vaccine efficacy against solid tumors in mice. *Cancer Immunol. Res.* **6**, 1301–1313 (2018).
23. S. Yang, Y. Traore, C. Jimenez, E. A. Ho, Autophagy induction and PDGFR-β knockdown by siRNA-encapsulated nanoparticles reduce chlamydia trachomatis infection. *Sci. Rep.* **9**, 1306 (2019).
24. J. Gu, S. Yang, E. A. Ho, Biodegradable film for the targeted delivery of siRNA-loaded nanoparticles to vaginal immune cells. *Mol. Pharm.* **12**, 2889–2903 (2015).
25. H. Hashemi, H. Varshosaz, H. Fazeli, S. M. Sharafi, H. Mirhendi, M. Chadeganipour, H. Yousefi, K. Manoochehri, Z. A. Chermahini, L. Jafarzadeh, N. Dehghanisamani, P. Dehghan, H. Y. Darani, Rapid differential diagnosis of vaginal infections using gold nanoparticles coated with specific antibodies. *Med. Microbiol. Immunol.* **208**, 773–780 (2019).
26. K. M. Fahrbach, O. Malykhina, D. J. Stieh, T. J. Hope, Differential binding of IgG and IgA to mucus of the female reproductive tract. *PLOS ONE* **8**, e76176 (2013).
27. H. K. Makadia, S. J. Siegel, Poly lactic-co-glycolic acid (PLGA) as biodegradable controlled drug delivery carrier. *Polymers* **3**, 1377–1397 (2011).
28. S. N. S. Alconcel, A. S. Baas, H. D. Maynard, FDA-approved poly(ethylene glycol)–protein conjugate drugs. *Polym. Chem.* **2**, 1442–1448 (2011).
29. E. Beltrán-Gracia, A. López-Camacho, I. Higuera-Ciapara, J. B. Velázquez-Fernández, A. A. Vallejo-Cardona, Nanomedicine review: Clinical developments in liposomal applications. *Cancer Nanotechnol.* **10**, 11 (2019).
30. S. Wang, J. Zhang, Y. Wang, M. Chen, Hyaluronic acid-coated PEI-PLGA nanoparticles mediated co-delivery of doxorubicin and miR-542-3p for triple negative breast cancer therapy. *Nanomedicine* **12**, 411–420 (2015).
31. S. Maiolino, A. Russo, V. Pagliara, C. Conte, F. Ungaro, G. Russo, F. Quaglia, Biodegradable nanoparticles sequentially decorated with Polyethyleneimine and Hyaluronan for the targeted delivery of docetaxel to airway cancer cells. *J. Nanobiotechnol.* **13**, 29 (2015).
32. U. F. and D. A. (FDA), Premarket Approval (PMA): Adherus AutoSpray Dural And ET Dural Sealant (2018).
33. S. K. Roy, B. Prabhakar, Bioadhesive polymeric platforms for transmucosal drug delivery systems – A review. *Trop. J. Pharm. Res.* **9**, 91–104 (2010).
34. J. W. McBride, N. Dias, D. Cameron, R. E. Offord, O. Hartley, P. Boyd, V. L. Kett, R. K. Malcolm, Pharmacokinetics of the protein microbicide 5P12-RANTES in sheep following single-dose vaginal gel administration. *Antimicrob Agents Chemother.* **61**, e00965-17 (2017).
35. R. M. Curran, L. Donnelly, R. J. Morrow, C. Fraser, G. Andrews, M. Cranage, K. R. Malcolm, R. J. Shattock, D. A. Woolfson, Vaginal delivery of the recombinant HIV-1 clade-C trimeric gp140 envelope protein CN54gp140 within novel rheologically structured vehicles elicits specific immune responses. *Vaccine* **27**, 6791–6798 (2009).
36. A. A. Date, A. Shibata, M. Goede, B. Sanford, K. L. Bruzzo, M. Belshan, C. J. Destache, Development and evaluation of a thermosensitive vaginal gel containing raltegravir + efavirenz loaded nanoparticles for HIV prophylaxis. *Antiviral Res.* **96**, 430–436 (2012).
37. T. Gong, Y. Hou, X. Yang, Y. Guo, Gelation of hydroxyethyl cellulose aqueous solution induced by addition of colloidal silica nanoparticles. *Int. J. Biol. Macromol.* **134**, 547–556 (2019).

38. D. Owen, D. Katz, A vaginal fluid simulant. *Contraception* **59**, 91–95 (1999).

39. D. Goode, R. Truong, G. Villegas, G. Calenda, N. Guerra-Perez, M. Piatak, J. D. Lifson, J. Blanchard, A. Gettie, M. Robbiani, E. Martinelli, HSV-2-driven increase in the expression of $\alpha_4\beta_7$ correlates with increased susceptibility to vaginal $SHIV_{SF162P3}$ infection. *PLOS Pathog.* **10**, e1004567 (2014).

40. S. Yang, Y. Chen, R. Ahmadie, E. A. Ho, Advancements in the field of intravaginal siRNA delivery. *J. Control. Release* **167**, 29–39 (2013).

41. L. M. Ensign, R. Cone, J. Hanes, Nanoparticle-based drug delivery to the vagina: A review. *J. Control. Release* **190**, 500–514 (2014).

42. J. K. Sheehan, I. Carlstedt, Hydrodynamic properties of human cervical-mucus glycoproteins in 6M-guanidinium chloride. *Biochem. J.* **217**, 93–101 (1984).

43. D. J. Thornton, D. F. Holmes, J. K. Sheehan, I. Carlstedt, Quantitation of mucus glycoproteins blotted onto nitrocellulose membranes. *Anal. Biochem.* **182**, 160–164 (1989).

44. J. K. Sheehan, K. Oates, I. Carlstedt, Electron microscopy of cervical, gastric and bronchial mucus glycoproteins. *Biochem. J.* **239**, 147–153 (1986).

45. F. Ceric, D. Silva, P. Vigil, Ultrastructure of the human periovulatory cervical mucus. *J. Electron. Microsc.* **54**, 479–484 (2005).

46. J. das Neves, M. Amiji, B. Sarmento, Mucoadhesive nanosystems for vaginal microbicide development: Friend or foe? *Wiley Interdiscip. Rev. Nanomed. Nanobiotechnol.* **3**, 389–399 (2010).

47. K. Yu, J. Zhao, C. Yu, F. Sun, Y. Liu, Y. Zhang, R. J. Lee, L. Teng, Y. Li, Role of four different kinds of polyethylenimines (PEIs) in preparation of polymeric lipid nanoparticles and their anticancer activity study. *J. Cancer* **7**, 872–882 (2016).

48. M. Arruebo, M. Valladares, Á. González-Fernández, Antibody-conjugated nanoparticles for biomedical applications. *J. Nanomater.* **2009**, 439389 (2009).

49. S. Kumar, J. Aaron, K. Sokolov, Directional conjugation of antibodies to nanoparticles for synthesis of multiplexed optical contrast agents with both delivery and targeting moieties. *Nat. Protoc.* **3**, 314–320 (2008).

50. M. K. Greene, D. A. Richards, J. C. F. Nogueira, K. Campbell, P. Smyth, M. Fernández, C. J. Scott, V. Chudasama, Forming next-generation antibody–nanoparticle conjugates through the oriented installation of non-engineered antibody fragments. *Chem. Sci.* **9**, 79–87 (2018).

51. K. A. Woodrow, Y. Cu, C. J. Booth, J. K. Saucier-Sawyer, M. J. Wood, W. M. Saltzman, Intravaginal gene silencing using biodegradable polymer nanoparticles densely loaded with small-interfering RNA. *Nat. Mater.* **8**, 526–533 (2009).

52. B. Poonia, L. Walter, J. Dufour, R. Harrison, P. A. Marx, R. S. Veazey, Cyclic changes in the vaginal epithelium of normal rhesus macaques. *J. Endocrinol.* **190**, 829–835 (2006).

53. S. Chen, J. Yi, B. Dong, C. Sun, P. F. Kiser, T. J. Hope, H. F. Zhang, Imaging endocervical mucus anatomy and dynamics in macaque female reproductive track using optical coherence tomography. *Quant. Imaging Med. Surg.* **5**, 40–45 (2015).

**Citation:** S. Yang, G. Arrode-Bruses, I. Frank, B. Grasperge, J. Blanchard, A. Gettie, E. Martinelli, E. A. Ho, Anti-$\alpha_4\beta_7$ monoclonal antibody–conjugated nanoparticles block integrin $\alpha_4\beta_7$ on intravaginal T cells in rhesus macaques. *Sci. Adv.* **6**, eabb9853 (2020).

# ScienceAdvances

**Anti-$\alpha_4\beta_7$ monoclonal antibody–conjugated nanoparticles block integrin $\alpha_4\beta_7$ on intravaginal T cells in rhesus macaques**

Sidi Yang, Geraldine Arrode-Bruses, Ines Frank, Brooke Grasperge, James Blanchard, Agegnehu Gettie, Elena Martinelli and Emmanuel A. Ho

| | |
|---|---|
| **ARTICLE TOOLS** | http://advances.sciencemag.org/content/6/34/eabb9853 |
| **REFERENCES** | This article cites 51 articles, 12 of which you can access for free<br>http://advances.sciencemag.org/content/6/34/eabb9853#BIBL |
| **PERMISSIONS** | http://www.sciencemag.org/help/reprints-and-permissions |

Use of this article is subject to the Terms of Service